Journal of Power Sources 193 (2009) 589–592

Contents lists available at ScienceDirect

Journal of Power Sources

journal homepage: www.elsevier.com/locate/jpowsour

Short communication

Low-temperature electrochemical characterization of dense ultra-thin lanthanum strontium cobalt ferrite ($La_{0.6}Sr_{0.4}Co_{0.8}Fe_{0.2}O_3$) cathodes synthesized by RF-sputtering on nanoporous alumina-supported Y-doped zirconia membranes

Hui Xiong [1], Bo-Kuai Lai, Alex C. Johnson, Shriram Ramanathan *

Harvard School of Engineering and Applied Sciences, Harvard University, Cambridge, MA 02138, United States

ARTICLE INFO

Article history:
Received 3 March 2009
Received in revised form 13 April 2009
Accepted 15 April 2009
Available online 23 April 2009

Keywords:
Lanthanum stronium cobalt ferrite
Solid oxide fuel cell
Cathode
Ultra-thin films
Nanocrystalline
Area-specific resistances
Microelectrode

ABSTRACT

Dense ultra-thin nanocrystalline $La_{0.6}Sr_{0.4}Co_{0.8}Fe_{0.2}O_3$ (LSCF) films with thickness of ~50 nm, have been sputtered on nanoporous anodic alumina-supported nanocrystalline thin film yttria-stabilized zirconia and patterned by photolithography into microelectrodes. This approach enables low-temperature (425–550 °C) electrochemical properties of dense ultra-thin nanocrystalline LSCF to be characterized. The results reveal that the electrochemical resistance of nanocrystalline ultra-thin LSCF is dominated by the oxygen surface exchange reaction at the electrode surface with an activation energy of 1.1 eV. Area-specific resistance of LSCF was obtained and the results are of potential relevance to utilizing nanostructured oxide cathodes for micro-SOFCs operated at low temperatures.

1. Introduction

Solid oxide fuel cells (SOFCs) convert chemical energy directly into electrical energy with advantages of high efficiency, low emission, and fuel flexibility [1]. Enormous efforts have been made to reduce their operating temperature from ~1000 °C down to intermediate (600–800 °C) and low (<600 °C) temperature range [2–5]. Due to thermally activated nature of ionic and electronic carriers [6,7], decrease in operating temperature is typically associated with ohmic resistive and polarization losses that eventually impairs the performance of SOFCs. This effect, however, can be compensated by decreasing electrolyte thickness [6], by choosing electrodes with higher electrocatalytic activity [7], by optimizing electrode microstructures [8], and by adopting mixed ionic and electronic conducting materials [7].

$La_{1-x}Sr_xCo_yFe_{1-y}O_{3-\delta}$ (LSCF) has been considered as one of the most promising cathodes for intermediate-temperature SOFCs due to its high mixed ionic and electronic conductivities and high electrocatalytic activity toward oxygen reduction reactions (ORR) [9,10]. LSCF in the form of thin films has recently been synthesized for μ-SOFCs [3,4] with a peak power density of ~60 mW cm^{-2} at 500 °C [4].

Polarization losses at the cathode are considered as a major limiting factor for SOFC performance, due to the sluggish ORR [7]. Therefore, understanding ORR processes at cathodes is of importance to improve SOFCs performance and geometrically well-defined thin film electrodes have been developed in recent years to investigate this problem quantitatively [8,11–14]. However, there are no reports regarding the low-temperature electrochemical properties of dense thin film LSCF cathodes synthesized by sputtering to the best of our knowledge.

In this paper, we report electrochemical measurements in the temperature range of 425–550 °C on dense ultra-thin films $La_{0.6}Sr_{0.4}Co_{0.8}Fe_{0.2}O_{3-\delta}$ synthesized by RF-sputtering. The ultra-thin film LSCF cathode is grown on a thin film nanocrystalline yttria-stabilized zirconia (YSZ) electrolyte supported by LSCF-coated nanoporous anodic alumina substrates. Area-specific resistances (ASRs), an important criterion for evaluation of cathode performance, are obtained in this study. Cracks in thin film electrodes can increase the area of the triple phase boundary (TPB) [7], which can complicate analysis of the ORR mechanism, therefore, crack-free ultra-thin LSCF films were ensured to validate the interpretation of electrochemical impedance data. To the best of our knowledge, this is the first report on low-temperature ASRs of RF-sputtered dense ultra-thin LSCF cathodes grown on thin film nanocrystalline YSZ of interest for solid oxide fuel cells.

* Corresponding author. Tel.: +1 617 496 0358; fax: +1 617 495 9837.
E-mail address: shriram@seas.harvard.edu (S. Ramanathan).
[1] Current address: Energy Systems Division, Argonne National Laboratory, 9700 South Cass Ave., Argonne, IL 60439, United States.

0378-7753/$ – see front matter © 2009 Elsevier B.V. All rights reserved.
doi:10.1016/j.jpowsour.2009.04.024

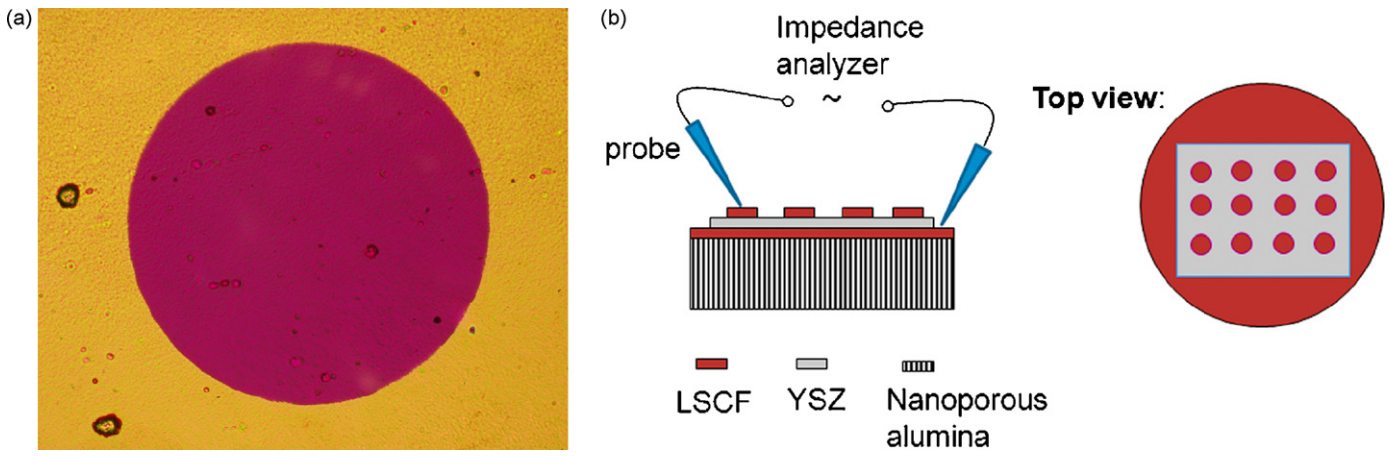

Fig. 1. Optical micrograph of a $La_{0.6}Sr_{0.4}Co_{0.8}Fe_{0.2}O_{3-\delta}$ microelectrode (purple circle) on a YSZ thin film grown on a nanoporous anodic alumina substrate (a); schematic of experimental arrangement (b). (For interpretation of the references to color in this figure legend, the reader is referred to the web version of the article.)

2. Experimental

The sample preparation procedure is described below: thin film counter electrode, electrolyte, and working electrode were deposited sequentially by RF-sputtering on a nanoporous anodic alumina substrate (Anodisc 13, Whatman, England). The area of the electrolyte was defined by a square shadow mask during sputtering. The working electrodes were patterned by photolithography into disk microelectrodes. A detailed description of each process step is described next: a 50-nm thick LSCF film was deposited on a nanoporous alumina substrate by RF-sputtering at 0.9 nm min^{-1} using a custom $La_{0.6}Sr_{0.4}Co_{0.8}Fe_{0.2}O_3$ target at a gun power of 60 W. A 200-nm thick YSZ film electrolyte was deposited by RF-sputtering through a shadow mask from a 8% Yttria-doped zirconia (AJA International) at a gun power of 100 W and an Ar pressure of 5 mTorr at 1.8 nm min^{-1}. Disk-shaped LSCF microelectrodes with nominal diameter of 200 μm were patterned by photolithography, RF-sputtering, and a lift-off process (Fig. 1a). Annealing of the samples was performed at 550 °C for 1 h in ambient in a Thermolyne 21100 tube furnace. Grazing incidence X-ray diffraction (XRD) was performed with a Scintag 2000 diffractometer using Cu Kα radiation. The thin films, surfaces and cross-section of the LSCF/YSZ/LSCF/alumina sample were investigated by a high resolution field emission SEM (Ultra55, Zeiss, Germany). The electrochemical impedance measurements were carried out using a Solartron SI 1260 impedance analyzer together with a Solartron SI 1287 Electrochemical Interface. The working and counter electrodes were contacted by Pt-plated tungsten tips positioned by micromanipulators connected to the impedance spectrometer to determine the ASRs (Fig. 1b). The impedances were measured at open circuit voltages (OCV) from 1 MHz to 0.01 Hz by applying a sinusoidal voltage with the amplitude of 20 mV, and measuring the corresponding current in the temperature range of 425–550 °C. The sample was placed on top of a homemade heating stage and measurements were performed in ambient condition. The temperature of the sample surface was measured using a K-type thermocouple placed directly above the sample surface.

3. Results and discussion

X-ray diffraction studies were carried out on a LSCF/YSZ/LSCF sample and the sample contains only YSZ and LSCF peaks and no crystalline interfacial reaction products were observed, consistent with our previous report on LSCF synthesis and crystallization studies [15].

Nanoporous anodic alumina substrates have been explored in recent studies to investigate fuel cell materials and structures [16,17]. These porous substrates allow free transport for the gases, and at the same time provide mechanical support for thin-film devices. In this study, we fabricated ultra-thin LSCF microelectrodes on thin film nanocrystalline YSZ electrolyte deposited on LSCF-sputtered nanoporous alumina substrates. The nanoporous alumina membrane is commercially available (Anodisc 13, Whatman) with a nominal pore size of 20 nm and a thickness of 60 μm. The structural analysis of such nanoporous substrate can be found in Refs. [18,19].

The morphology and microstructure of the thin films were investigated by SEM. Fabrication of a crack-free films is crucial in elucidating the mechanism at dense thin-film mixed-conducting electrodes because cracks can introduce additional surface area and thus changes to behavior more like a porous electrode [7]. Moreover, cracks in thin films with a free-standing configuration for μ-SOFCs could have deteriorative effect such as rupturing the thin film membranes. Therefore, obtaining crack-free thin films is important for our purpose to understand the polarization loss at the LSCF thin film cathode used for μ-SOFCs. The SEM images shown in Fig. 2a reveal that the LSCF thin film (~50 nm thick) is conformal, dense and continuous. No evidence for cracks was found in the entire region under investigation. The grain size of the annealed (550 °C for 1 h) thin films was estimated to be ~50 nm (Fig. 2b).

Fig. 2c shows the SEM image of the surface of the YSZ thin film on LSCF-sputtered anodic alumina substrate. The YSZ film is nanocrystalline, smooth, continuous, and crack-free over the whole region as well. The cross-sectional SEM image shown in Fig. 2d indicates the 50-nm thick LSCF film completely covers the nanoporous substrate and the YSZ film of thickness nearly 200 nm is dense to form a gas-tight electrolyte layer.

Due to experimental limitations, there are only few prior reports describing thin film $(LaSr)(CoFe)O_{3-\delta}$ cathode behavior at or below 600 °C [12,20]. By a suitable combination of thin film structures on nanoporous substrates we have been able to determine ASRs of LSCF at temperatures as low as 425 °C. Nanocrystalline thin film YSZ electrolyte with thickness ~200 nm was used throughout the measurements. The size of the LSCF microelectrode (200 μm) is about 1000 times of the thickness of the electrolyte, therefore due to the effect of current constriction [7,14] the LSCF/YSZ/LSCF configuration used in this study is similar to a symmetrical cell.

Fig. 3a shows the impedance data of the LSCF/YSZ/LSCF cell as a function of temperature (425–550 °C). There are three representative features in the spectra (see inset, Fig. 3a) within the

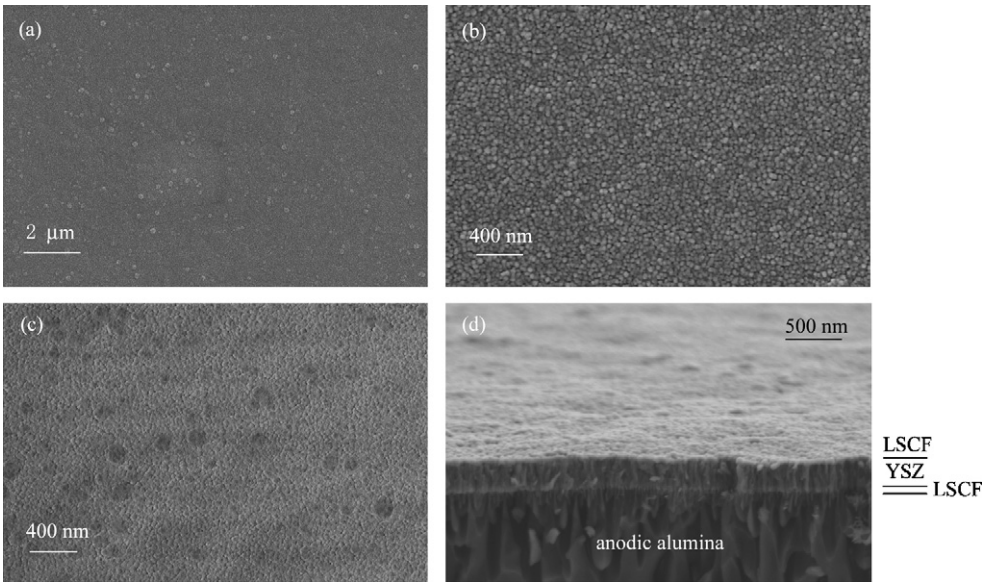

Fig. 2. Scanning electron microscopic images of the surface of the sputtered LSCF thin film with large view (a) and close view (b); sputtered YSZ thin film (c), and cross-sectional view of LSCF/YSZ/LSCF on nanoporous alumina substrate (d).

temperature range studied: one dominating almost "ideal" semicircle at low frequency (LF), one depressed semicircle at medium frequency (MF), and a non-zero axis intercept at high frequency (HF). The experimental data were fitted by equivalent circuit model (Fig. 3b), where a general constant phase element (CPE) was chosen to denote non-ideal semicircles. The impedance of such a CPE is given by $Z_{CPE} = [Q(i\omega)^n]^{-1}$, with Q and n as fitting parameters. For the LF feature, the n values are very close to 1 (>0.96) in the whole temperature range, whereas the MF feature is less ideal ($n \sim 0.7$).

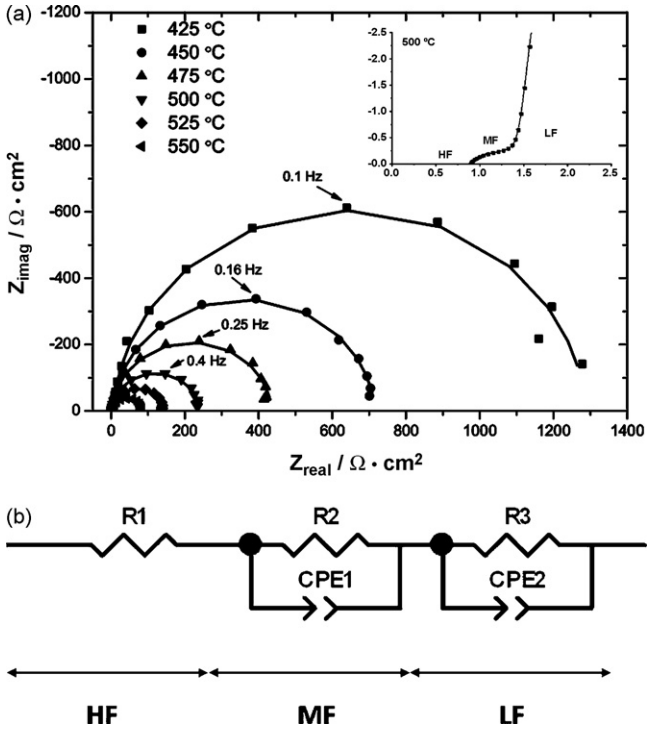

Fig. 3. Nyquist plots from a LSCF/YSZ/LSCF cell on a nanoporous anodic alumina substrate measured in air as a function of temperature (a). Symbols: experimental data; solid lines: fitted curves based on equivalent circuit model (b). The inset shows the enlarged view of high frequency and medium frequency parts of a spectrum recorded at 500 °C.

The fitted curves correspond with the experimental data very well over the whole frequency and temperature range measured.

R_1 at HF is mostly attributed to the ohmic resistance of the electrolyte, sheet resistance of electrode surface, and electrical contacts from the probes. The small semicircle at MF likely originates from the electrolyte/electrode interface from previous studies with similar dense (LaSr)(CoFe)$O_{3-\delta}$ thin film electrode on YSZ systems [13,21,22]. This process is thermally activated (Fig. 4) and disappears at higher temperature (>550 °C). The activation energy of 1.34 eV extracted from the Arrhenius plot is in agreement with literature values [12,13].

The electrode process at LF can be attributed to oxygen surface exchange reaction [12,13,21–23]. The LSCF film thickness (50 nm) is much smaller than the characteristic thickness ($Lc = D^*/k^*$) [23], which indicates that surface exchange process is rate-limiting rather than bulk diffusion pathways. Lc is known to be ~100 μm for the mixed conducting perovskite oxide family of (LaSr)(CoFe)$O_{3-\delta}$ [23]. The activation energy of R_3 (1.1 eV) is consistent with literature data for dense thin films of similar composition [12,13,21].

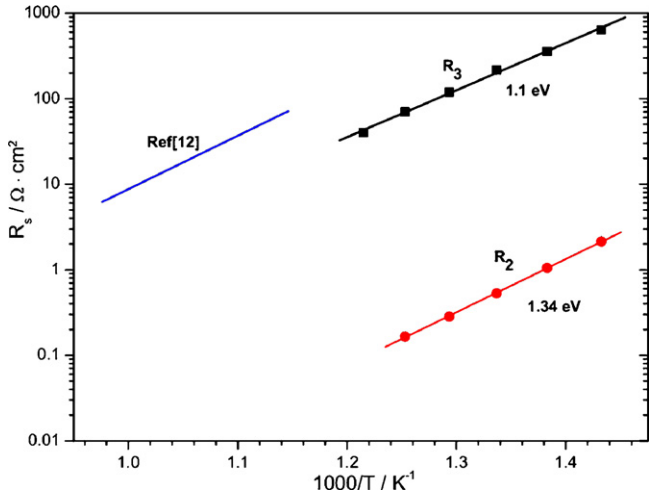

Fig. 4. Surface (R_3) and interfacial (R_2) ASRs as a function of temperature between 425 and 550 °C. Blue solid line: temperature dependence of surface ASRs from Ref. [12]. (For interpretation of the references to color in this figure legend, the reader is referred to the web version of the article.)

The ASRs of sputtered LSCF from this study are lower compared to the literature from direct extrapolation (Fig. 4), which is potentially encouraging towards their application as cathodes for low-temperature fuel cells. Such differences could arise from differences in microstructure or synthesis routes. In order to evaluate the current constriction effects on impedance response, we estimated the J value, a dimensionless factor described in Ref. [7]. This works out to be much smaller than 1 and indicates negligible effect on interpretation of electrode impedance. The Anodisc support blocks a small fraction of the bottom electrode but may also increase active area due to LSCF deposition inside the pores of the Anodisc. We anticipate this to only have a minimal impact in our results. The chemical capacitance [7] obtained from the LF features within the experimental temperature range are nearly constant and are $\sim$1.3 mF cm^{-2}. This indicates that the LSCF cathode here undergoes minimal changes in stoichiometry at temperatures below 550 °C since chemical capacitance is an indicator of the readiness for such changes [7].

4. Conclusion

We have performed low-temperature electrochemical characterization of dense ultra-thin film sputtered LSCF cathodes for SOFC. The LSCF thin films were fabricated into lithographically patterned disk microelectrodes. The process at the cathode is a thermally activated surface exchange reaction with an activation barrier of 1.1 eV. The nearly constant chemical capacitance indicates the cathode undergoes minor change in stoichiometry under these conditions. The results suggest potential for sputtered oxide cathodes in low-temperature solid oxide fuel cells.

Acknowledgment

The authors acknowledge financial support from Harvard University SEAS, SiEnergy Systems and University Center for Environment.

References

[1] S.M. Haile, Acta Mater. 51 (2003) 5981–6000.
[2] H. Huang, M. Nakamura, P.C. Su, R. Fasching, Y. Saito, F.B. Prinz, J. Electrochem. Soc. 154 (2007) B20–B24.
[3] A. Bieberle-Hutter, D. Beckel, A. Infortuna, U.P. Muecke, J.L.M. Rupp, L.J. Gauckler, S. Rey-Mermet, P. Muralt, N.R. Bieri, N. Hotz, M.J. Stutz, D. Poulikakos, P. Heeb, P. Muller, A. Bernard, R. Gmur, T. Hocker, J. Power Sources 177 (2008) 123–130.
[4] A.C. Johnson, B.-K. Lai, H. Xiong, S. Ramanathan, J. Power Sources 186 (2009) 252–260.
[5] C. Peters, A. Weber, E. Ivers-Tiffee, J. Electrochem. Soc. 155 (2008) B730–B737.
[6] B.C.H. Steele, A. Heinzel, Nature 414 (2001) 345–352.
[7] S.B. Adler, Chem. Rev. 104 (2004) 4791–4843.
[8] A. Bieberle-Hutter, M. Sogaard, H.L. Tuller, Solid State Ionics 177 (2006) 1969–1975.
[9] A. Esquirol, N. Brandon, J. Kilner, M. Mogensen, J. Electrochem. Soc. 151 (2004) A1847–A1855.
[10] D. Beckel, U.P. Muecke, T. Gyger, G. Florey, A. Infortuna, L.J. Gauckler, Solid State Ionics 178 (2007) 407–415.
[11] V. Brichzin, J. Fleig, H.U. Habermeier, J. Maier, Electrochem. Solid State Lett. 3 (2000) 403–406.
[12] F.S. Baumann, J. Fleig, G. Cristiani, B. Stuhlhofer, H.U. Habermeier, J. Maier, J. Electrochem. Soc. 154 (2007) B931–B941.
[13] F.S. Baumann, J. Fleig, H.U. Habermeier, J. Maier, Solid State Ionics 177 (2006) 1071–1081.
[14] J. Fleig, F.S. Baumann, V. Brichzin, H.R. Kim, J. Jamnik, G. Cristiani, H.U. Habermeier, J. Maier, Fuel Cells 6 (2006) 284–292.
[15] B.-K. Lai, A.C. Johnson, H. Xiong, S. Ramanathan, J. Power Sources 186 (2009) 115–122.
[16] Y.I. Park, P.C. Su, S.W. Cha, Y. Saito, F.B. Prinz, J. Electrochem. Soc. 153 (2006) A431–A436.
[17] J.H. Joo, G.M. Choi, Solid State Ionics 178 (2007) 1602–1607.
[18] Y.I. Park, S.W. Cha, Y. Saito, F.B. Prinz, Thin Solid Films 476 (2005) 168–173.
[19] S. Kang, P.C. Su, Y.I. Park, Y. Saito, F.B. Prinz, J. Electrochem. Soc. 153 (2006) A554–A559.
[20] M. Prestat, A. Infortuna, S. Korrodi, S. Rey-Mermet, P. Muralt, L.J. Gauckler, J. Electroceram. 18 (2007) 111–120.
[21] Y.L. Yang, C.L. Chen, S.Y. Chen, C.W. Chu, A.J. Jacobson, J. Electrochem. Soc. 147 (2000) 4001–4007.
[22] A. Ringued, J. Fouletier, Solid State Ionics 139 (2001) 167–177.
[23] B.C.H. Steele, Solid State Ionics 75 (1995) 157–165.